LUND UNIVERSITY

Estimation of depth of fluorescing lesions in tissue from changes in fluorescence spectra

Swartling, Johannes; Bengtsson, D; Terike, K; Svensson, Jenny; Andersson-Engels, Stefan

Link to publication

Estimation of depth of fluorescing lesions in tissue from changes in fluorescence spectra

Johannes Swartling, Daniel Bengtsson, Khaled Terike, Jenny Svensson, Stefan Andersson-Engels

Lund University Medical Laser Centre, Dept. of Physics, Lund Institute of Technology. P.O. Box 118, SE-221 00 Lund, Sweden. E-mail: Johannes.Swartling@fysik.lth.se, Stefan.Andersson-Engels@fysik.lth.se

ABSTRACT

We present a novel method for estimating the depth of a fluorescent lesion in tissue based on measurements of the fluorescence signal in different wavelength bands. The measured fluorescence spectrum following irradiation by excitation light at the surface is a function of several parameters, because the fluorescence light has to pass through tissue with characteristic scattering and absorption properties. Thus, the intrinsic fluorescence spectrum will be altered, in a way determined by the tissue optical properties, the depth of the fluorophore, and also by the geometry of the light irradiation and the detection system. By analyzing the ratio between the signals at two wavelengths we show that it is possible to estimate the depth of the lesion. We have performed Monte Carlo simulations and measurements on an Intralipid phantom in the wavelength range 850 - 1000 nm. By taking the ratio between the signals at the wavelengths 875 and 930 nm the depth of a fluorescing layer could be determined with 0.8 mm accuracy down at least a depth of 10 mm. Monte Carlo simulations were also performed for different tissue types with various composition. The results indicate that depth estimation of a lesion is possible with no assumptions made about the optical properties for a wide range of tissues.

Keywords: fluorescence, spectroscopy, photon migration, turbid media

1. INTRODUCTION

The interest is growing quickly in fluorescence measurements of embedded structures for tissue diagnostics. The principle is based on techniques where the tissue is irradiated with excitation light and the emitted fluorescence signal is detected on the surface. The fluorescence signal contains information about the concentration and distribution of the fluorophore inside the tissue. This approach has the potential to discriminate tumors inside the tissue, provided that the fluorophore is selectively targeting the tumor.

Fluorescence techniques can be used to reach deep into tissue by using excitation wavelengths approximately within the 600-900 nm range, partly because of lower scattering, and partly due to the lower absorption in this region. Intense research is being carried out to develop cancer diagnostics using fluorophores which have long excitation wavelengths in the red or near infrared (NIR) region. This enables fluorescence emission from deep structures, in the order of several centimeters [1,2]. A specific application that has been suggested is detection of sentinel nodes in cancer patients [3,4]. Fluorescence-based detection could be a simpler and safer alternative to the current method based on injection of radio-isotopes. Other applications include measurements of the fluorescence from photosensitizers for photodynamic therapy, where the aim is to optimize treatment parameters and monitor photobleaching of the drug [5,6].

In this paper we study the problem of determining depth of fluorescent lesions in tissue. The shape of the fluorescence spectrum from an embedded lesion is influenced by the depth of the lesion, due to the fact that the fluorescence light is filtered when migrating through the tissue to the surface. This filtering occurs as a result of the intrinsic scattering and absorption properties of the tissue. Thus, we investigate the potential of using changes in the fluorescence spectra to estimate the depth, d, of a fluorescing lesion in a semi-infinite volume.

The method we describe relies on the fact that the absorption coefficient of the tissue is non-uniform over the spectral region of fluorescence emission, with the result that relative spectral intensities change for different wavelength bands as the fluorescence light propagates to the surface. The changes can serve as a measure of the depth of the fluorophore. Our approach is to form the ratio between the measured fluorescence signals at two wavelengths λ_1 and λ_2,

$$\gamma = \frac{\Gamma(\lambda_1)}{\Gamma(\lambda_2)} \tag{1}$$

where Γ is the probability of detecting a fluorescence photon. The next step is to evaluate the dependence of γ on d. One of the advantages with this approach is that by forming a ratio there is no need for absolute measurements of the fluorescence light, and some uncontrolled parameters cancel out. We have performed Monte Carlo simulations of excitation and fluorescence light to prove the principle of this approach. The simulation results were then directly compared with the results from measurements performed on a tissue phantom to provide experimental verification of the method. We also performed a series of Monte Carlo simulations with realistic tissue optical properties, for various tissue types, to assess the robustness of the method with respect to biological variability.

2. MATERIAL AND METHODS

2.1 Monte Carlo Simulations

We have previously developed a Monte Carlo method for simulating fluorescence from layered tissues [7]. In brief, this method takes advantage of symmetry aspects to reduce the computation time. In addition, we split the simulation of the excitation light and the emission light into two separate problems. The resulting data sets are convolved to provide the final answer. The efficiency is increased even further by applying a reciprocity theorem for the calculation of the emission light, which effectively reverses the photon paths of the fluorescence light, so that only one simulation is needed, with the source of photons placed at the surface. We showed that for certain applications the computation time could be reduced by two orders of magnitude or more using these techniques, compared to the conventional method for simulating fluorescence [7]. The Monte Carlo code is time-resolved which enables studies of the effects of fluorophore lifetimes and photon migration time dispersion.
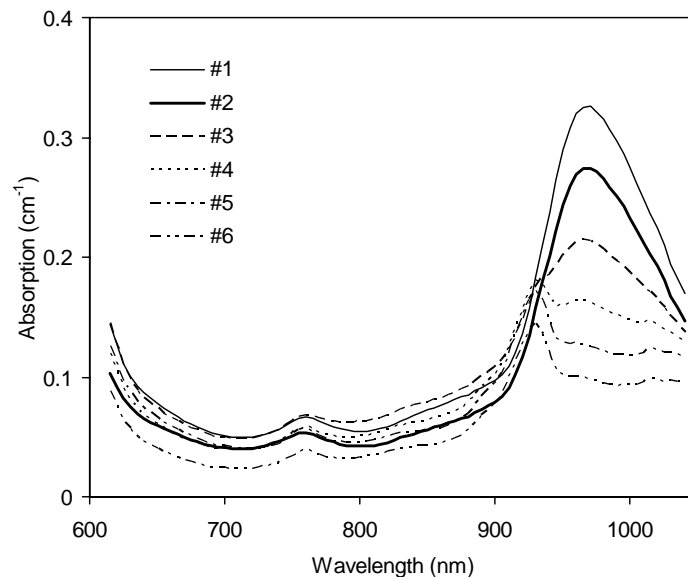

Figure 1. Optical properties of six different types of breast tissue (from Pifferi et al.[8]). The absorption spectra represent fitted curves rather than actual measurement data.
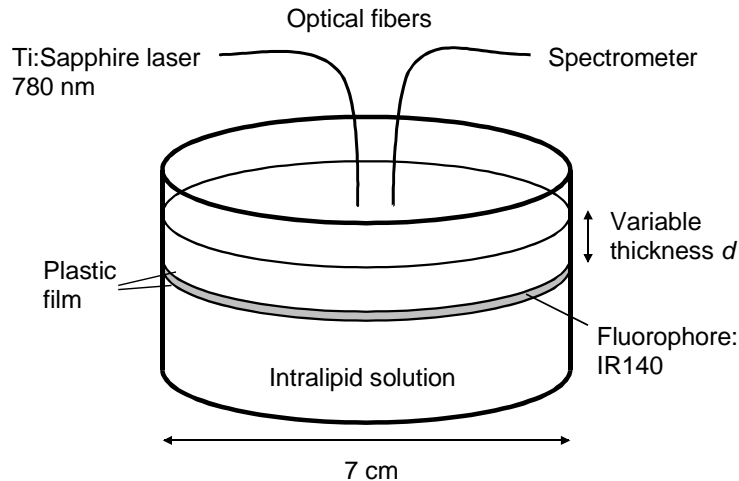
Figure 2. Schematic of phantom and set-up.

To validate the simulations experimentally, we performed Monte Carlo simulations with optical properties similar to phantoms, whose optical properties were measured independently using an integrating-sphere method [9].

Simulations were also performed with optical properties similar to those in real tissue. For this, we used absorption spectra for tissue based on data from previous measurements of breast tissue, where the dominant absorbers in the red and near infrared region are water, fat, and deoxygenated and oxygenated hemoglobin [8]. The absorption spectra that were used in the simulations are shown in Fig. 1. The tissue types were ranging from water rich (62% water, 16% lipid for #1) to lipid rich (12% water, 68% lipid for #6), and thus represent a very wide span in terms of different tissue types.

2.2 Phantom

In order to demonstrate the differences in fluorescence spectrum from a lesion at different depths we developed a phantom with an embedded inclusion at a variable depth d. The phantom was made from 1 part Intralipid-20% (Fresenius Kabi, Sweden) and 21 parts water. It consisted of three layers, as depicted in Fig. 2, where the upper and lower layers had the same optical properties, and black ink was added to provide background absorption (2.3 µl/l). We separated the middle layer, which was 1 mm thick, by using thin plastic foil. A fluorescent dye (IR-140, Exciton, USA) was added to this layer. We could easily vary the depth of the upper layer, d, by adding or removing the liquid.

We determined the optical properties of the phantom by using an integrating sphere [9]. We used a cuvette made of glass slides, which gave a sample thickness of 1.00 mm and lateral dimensions of 3×3 cm. The integrating sphere set-up was used to measure the total transmission, total reflectance, and collimated transmittance. The optical properties – μ_a, μ_s, and the scattering anisotropy factor g – were evaluated by using Monte Carlo look-up tables [9].

2.3 Fluorescence Measurements

A Ti:Sapphire laser at 780 nm was used as excitation source for the phantom. The power was limited to about 10 mW. The light was guided to the phantom surface by using a 400-µm core diameter step index fiber (NA=0.22), and another fiber collected the fluorescence light and guided it to a spectrometer (HoloSpec f/1.8i, Kaiser Optical Systems, USA). The laser wavelength was removed with a long-pass filter. For detection, a cooled CCD camera (LN/CCD-1024-EERB/1, Princeton Instruments, USA) was used. We acquired fluorescence spectra over the range 815-930 nm.
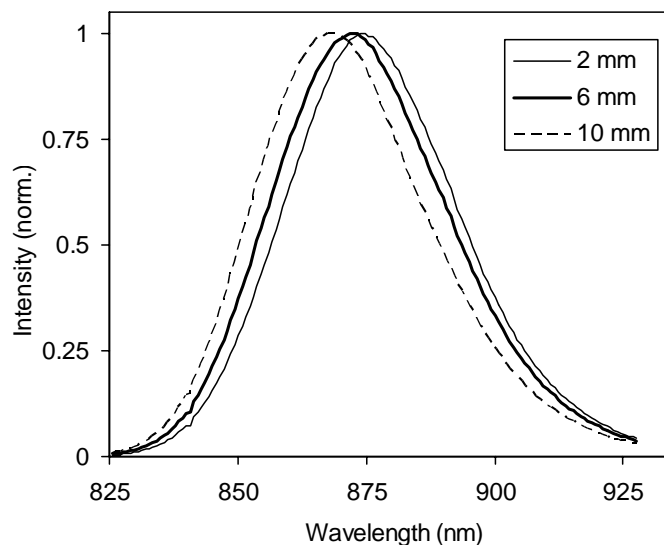
Figure 3. Measured (normalized) fluorescence spectra for different depths of the layer with fluorescing IR 140: 2, 6 and 10 mm.

3. RESULTS

3.1 Phantom Measurements and Simulations

We used the optical properties of the phantom as determined by the integrating sphere method as input for the Monte Carlo simulations. The anisotropy factor g was around 0.65 over the wavelength range. Measured fluorescence spectra at different depths are presented in Fig. 3, which shows a wavelength shift of the spectrum as the depth increases. In the Monte Carlo simulations, the highest value of the ratio γ was obtained with $\lambda_1=815$ nm and $\lambda_2=960$ nm. However, the fluorescence signal was low at long wavelengths so we had to use a shorter λ_2 to obtain a good signal-to-noise ratio from the measurements. In Fig. 4 we present γ as a function of d for $\lambda_1=886$ nm and $\lambda_2=922$ nm.

By using the simulation results as a calibration curve, we also attempted to predict the depth of the fluorophore from the experimental values of γ. We then calculated the differences between the predicted and the true values of d, which resulted in a standard deviation in the predicted values of 0.6 mm.

3.2 Monte Carlo Simulations of Tissue

Simulations were repeated for six different sets of tissue optical properties to account for typical biological variability of the tissue composition, as was presented in Fig. 1. We assumed that the excitation wavelength was 615 nm, and the fluorescence was simulated in the region 625-1005 nm in steps of 10 nm. For each individual simulation, i.e., one wavelength and one set of tissue optical properties, 5×10^5 photon histories were traced. The fluorescing lesion was simulated as a 1 mm thick layer. We varied the depth of the upper layer to the lesion from 0 to 10 mm.

The first task was to investigate the wavelengths where the ratios are the largest and thus best suited for evaluating the depth of the fluorophore. To determine the optimal choice of wavelengths for the method we plotted $d\gamma/dd$ for $625<\lambda_1,\lambda_2<1005$ nm. The initial results showed that $\gamma(d)$ was approximately linear, so we used $d\gamma/dd$ determined by the slope of a regression line. The results are presented in Fig. 5, for tissue type #1 (a) and #6 (b). The points with the largest values in these plots may be interpreted as corresponding to the best wavelength choices in terms of obtaining a high ratio.
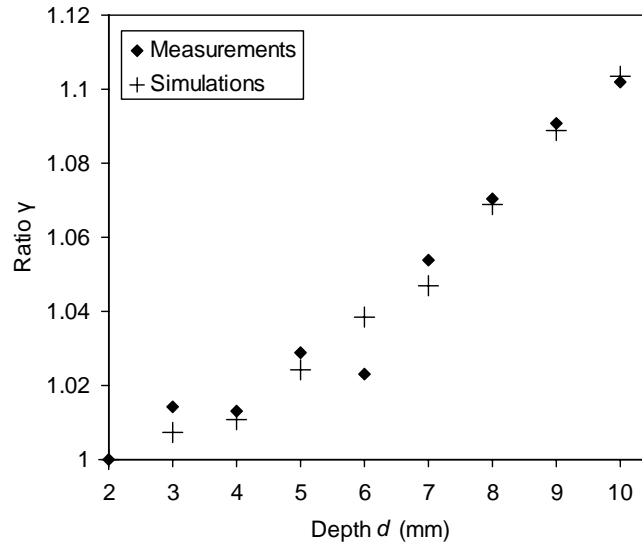
Figure 4. The ratio γ shown for $\lambda_1 = 886$ nm and $\lambda_2 = 922$ nm, as a function of the depth d. Results from both measurements on the Intralipid phantom and the Monte Carlo simulations are shown.
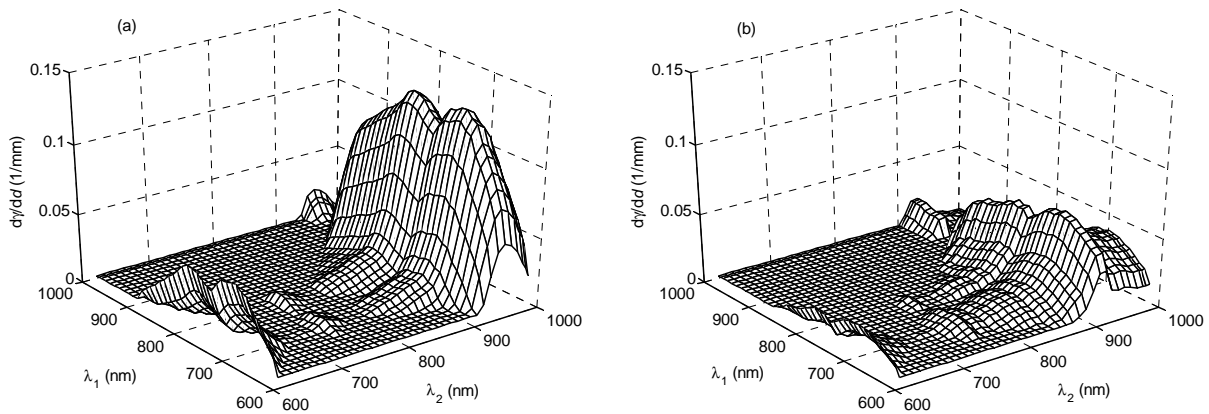

Figure 5. Plots showing $d\gamma/dd$ as a function of λ_1 and λ_2. Only values where $\gamma>1$ are plotted. (a) Tissue type #1, water rich. (b) Tissue type #6, lipid rich.

By analyzing $d\gamma/dd$, it is also possible to assess how robustly the ratios correspond to a given depth for different tissue types. This was done by searching for the λ_1-λ_2-pair that gives the least variation in $d\gamma/dd$ for all six tissue types. We also wanted $d\gamma/dd$ to be relatively high, and this resulted in the best wavelengths $\lambda_2=935$ nm, with $\lambda_1=695$ nm, $\lambda_1=745$-755 nm, or $\lambda_1=875$ nm. At $(\lambda_1,\lambda_2)=(695$ nm,935 nm), the mean value was $d\gamma/dd=0.063$ mm^{-1}, with a standard deviation of 0.005 mm^{-1}. At $(\lambda_1,\lambda_2) = (875$ nm,935 nm), the mean value was $d\gamma/dd=0.043$ mm^{-1}, with a standard deviation of 0.005 mm^{-1}. Next, we applied these values to predict d from the simulation of each of the six tissue types. The results are shown in Fig. 6(a) for $(\lambda_1,\lambda_2)=(695$ nm,935 nm), and in Fig. 6(b) for $(\lambda_1,\lambda_2)=(875$ nm,935 nm). In Fig. 6(a), most of the predicted values of d are within 1.5 mm of the true value, except for the most water rich tissue type (#1) which consistently overestimates the depth by about 2-2.5 mm. In Fig. 6(b), the largest errors occur for tissue types #2 and #6, which are underestimated by up to 2 mm.
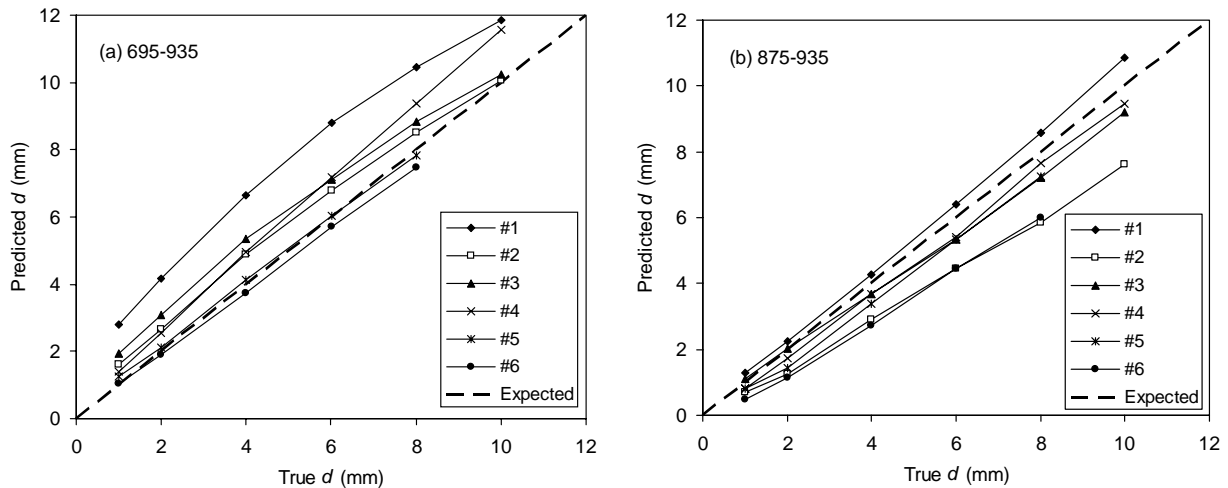
Figure 6. Values of the depth d predicted from the Monte Carlo simulations for each of the six different tissue types. In all six cases the same calibration was used. (a) Calibration based on the mean value $d\gamma/dd$=0.063 mm^{-1} at (λ_1,λ_2)=(695 nm,935 nm). (b) Calibration based on the mean value $d\gamma/dd$=0.043 mm^{-1} at (λ_1,λ_2)=(875 nm,935 nm).

4. DISCUSSION

The results from the Monte Carlo simulations show that the ratio $\gamma(\lambda_1,\lambda_2)$ is a useful indicator of the depth of a fluorescing lesion, given that one uses the right combinations of wavelengths λ_1 and λ_2. The phantom measurements confirm the simulations and demonstrate the feasibility of the method using a relatively simple experimental set-up. In the case of the phantom we utilize the difference in water absorption at the slope of the vibrational overtone band that has a maximum absorption at 970 nm. We used λ_2=922 nm, although a longer wavelength would have given a higher ratio γ; we were however limited to about 930 nm by the fact that the fluorescence spectrum for IR-140 drops to low intensity for longer wavelengths. The depth of the fluorescing layer was recovered from the experimental data with an accuracy of 0.6 mm.

For real tissue there are two regions that are potentially useful for choosing the wavelengths λ_1 and λ_2. One can use the same slope of the water absorption band above 900 nm as discussed above, or the slope of the hemoglobin absorption in the 600-650 nm region. The analysis of the plots in Fig. 5 indicated that that choosing (λ_1, λ_2)=(695 nm,935 nm) or (λ_1, λ_2)=(875 nm,935 nm) would be optimal. Using $\lambda_2 \approx 930$ is useful in this respect because this is a quasi-isosbestic point where the variation between various soft tissues is minimal, owing to the fact that the absorption spectra of lipid and water cross at this wavelength [8]. This makes the prediction of the depth somewhat insensitive to the tissue composition. With λ_a=695 nm we could recover the depth of the layer with an error of less than 1.5 mm for all tissue types except the most water rich (tissue type #1). When considering the large differences in tissue composition and thus optical properties between the six tissue types, such good prediction accuracy is very encouraging. Using the wavelength pair (λ_1, λ_2)=(695 nm,935 nm) may be difficult in practice, due to the difficulty in finding a suitable fluorophore with such a wide emission spectrum. Using the wavelengths (λ_1, λ_2)=(875 nm,935 nm) is a better alternative, and the results in Fig. 6(b) show that the depth prediction accuracy for these wavelengths is similar.

With the proposed method, we see a potential application based on a probe delivering excitation light and at the same time detecting the fluorescence light by means of relatively simple photodetectors and wavelength-selecting filters. We also consider our method promising in terms of providing depth information for image fluorometry and molecular imaging, as a technique to resolve the fluorophore distribution in three dimensions.

ACKNOWLEDGMENTS

REFERENCES

1. V. Ntziachristos, J. Ripoll, R. Weissleder, "Would near-infrared fluorescence signals propagate through large human organs for clinical studies?" Opt. Lett. 27, 333-335 (2002)
2. V. Ntziachristos, C-H. Tung, C. Bremer, R. Weissleder, "Fluorescence molecular tomography resolves protease activity in vivo", Nature Medicine 8, 757-760 (2002)
3. J.S. Reynolds, T.L. Troy, R.H. Mayer, A.B. Thompson, D.J. Waters, K.K. Cornell, P.W. Snyder, and E.M. Sevick-Muraca, "Imaging of spontaneous canine mammary tumors using fluorescent contrast agents," Photochem Photobiol 70, 87-94 (1999)
4. A. Eidsath, V. Chernomordik, A.H. Gandjbakhche, P. Smith, and A. Russo, "Three-dimensional localization of fluorescent masses deeply embedded in tissue," Phys.Med.Biol. 47, 4079-4092 (2002)
5. TJ Farrell, RP Hawkes, MS Patterson and BC Wilson, "Modeling of photosensitizer fluorescence emission and photobleaching for photodynamic therapy dosimetry", Appl Opt 37, 7168-83 (1998)
6. T. Johansson, M. Soto Thompson, M. Stenberg, C. af Klinteberg, S. Andersson-Engels, S. Svanberg, and K. Svanberg, "Feasibility study of a novel system for combined light dosimetry and interstitial photodynamic treatment of massive tumors," Appl.Opt. 41, 1462-1468 (2002)
7. J. Swartling, A. Pifferi, A.M.K. Enejder, and S. Andersson-Engels, "Accelerated Monte Carlo model to simulate fluorescence spectra from layered tissues," J.Opt.Soc.Am.A 20, 714-727 (2003)
8. A. Pifferi, J. Swartling, E. Chikoidze, A. Torricelli, P. Taroni, A. Bassi, S. Andersson-Engels, and R. Cubeddu, "Spectroscopic time-resolved diffuse reflectance and transmittance measurements of the female breast at different interfiber distances," J Biomed Opt 9, 1143-1151 (2004)
9. J. Swartling, J.S. Dam, and S. Andersson-Engels, "Comparison of spatially and temporally resolved diffuse-reflectance measurement systems for determination of biomedical optical properties," Appl.Opt. 42, 4612-4620 (2003)